Observation of two resonant structures in $e^+e^- \to \pi^+\pi^- h_c$

M. Ablikim[1], M. N. Achasov[9,e], S. Ahmed[14], X. C. Ai[1], O. Albayrak[5], M. Albrecht[4], D. J. Ambrose[44], A. Amoroso[49A,49C], F. F. An[1], Q. An[46,a], J. Z. Bai[1], O. Bakina[23], R. Baldini Ferroli[20A], Y. Ban[31], D. W. Bennett[19], J. V. Bennett[5], N. Berger[22], M. Bertani[20A], D. Bettoni[21A], J. M. Bian[43], F. Bianchi[49A,49C], E. Boger[23,c], I. Boyko[23], R. A. Briere[5], H. Cai[51], X. Cai[1,a], O. Cakir[40A], A. Calcaterra[20A], G. F. Cao[1], S. A. Cetin[40B], J. Chai[49C], J. F. Chang[1,a], G. Chelkov[23,c,d], G. Chen[1], H. S. Chen[1], J. C. Chen[1], M. L. Chen[1,a], S. Chen[41], S. J. Chen[29], X. Chen[1,a], X. R. Chen[26], Y. B. Chen[1,a], X. K. Chu[31], G. Cibinetto[21A], H. L. Dai[1,a], J. P. Dai[34], A. Dbeyssi[14], D. Dedovich[23], Z. Y. Deng[1], A. Denig[22], I. Denysenko[23], M. Destefanis[49A,49C], F. De Mori[49A,49C], Y. Ding[27], C. Dong[30], J. Dong[1,a], L. Y. Dong[1], M. Y. Dong[1,a], Z. L. Dou[29], S. X. Du[53], P. F. Duan[1], J. Z. Fan[39], J. Fang[1,a], S. S. Fang[1], X. Fang[46,a], Y. Fang[1], R. Farinelli[21A,21B], L. Fava[49B,49C], F. Feldbauer[22], G. Felici[20A], C. Q. Feng[46,a], E. Fioravanti[21A], M. Fritsch[14,22], C. D. Fu[1], Q. Gao[1], X. L. Gao[46,a], Y. Gao[39], Z. Gao[46,a], I. Garzia[21A], K. Goetzen[10], L. Gong[30], W. X. Gong[1,a], W. Gradl[22], M. Greco[49A,49C], M. H. Gu[1,a], Y. T. Gu[12], Y. H. Guan[1], A. Q. Guo[1], L. B. Guo[28], R. P. Guo[1], Y. Guo[1], Y. P. Guo[22], Z. Haddadi[25], A. Hafner[22], S. Han[51], X. Q. Hao[15], F. A. Harris[42], K. L. He[1], F. H. Heinsius[4], T. Held[4], Y. K. Heng[1,a], T. Holtmann[4], Z. L. Hou[1], C. Hu[28], H. M. Hu[1], J. F. Hu[49A,49C], T. Hu[1,a], Y. Hu[1], G. S. Huang[46,a], J. S. Huang[15], X. T. Huang[33], X. Z. Huang[29], Z. L. Huang[27], T. Hussain[48], W. Ikegami Andersson[50], Q. Ji[1], Q. P. Ji[15], X. B. Ji[1], X. L. Ji[1,a], L. W. Jiang[51], X. S. Jiang[1,a], X. Y. Jiang[30], J. B. Jiao[33], Z. Jiao[17], D. P. Jin[1,a], S. Jin[1], T. Johansson[50], A. Julin[43], N. Kalantar-Nayestanaki[25], X. L. Kang[1], X. S. Kang[30], M. Kavatsyuk[25], B. C. Ke[5], P. Kiese[22], R. Kliemt[10], B. Kloss[22], O. B. Kolcu[40B,h], B. Kopf[4], M. Kornicer[42], A. Kupsc[50], W. Kühn[24], J. S. Lange[24], M. Lara[19], P. Larin[14], L. Lavezzi[49C,1], H. Leithoff[22], C. Leng[49C], C. Li[50], Cheng Li[46,a], D. M. Li[53], F. Li[1,a], F. Y. Li[31], G. Li[1], H. B. Li[1], H. J. Li[1], J. C. Li[1], Jin Li[32], K. Li[13], K. Li[33], Lei Li[3], P. R. Li[7,41], Q. Y. Li[33], T. Li[33], W. D. Li[1], W. G. Li[1], X. L. Li[33], X. N. Li[1,a], X. Q. Li[30], Y. B. Li[2], Z. B. Li[38], H. Liang[46,a], Y. F. Liang[36], Y. T. Liang[24], G. R. Liao[11], D. X. Lin[14], B. Liu[34], B. J. Liu[1], C. X. Liu[1], D. Liu[46,a], F. H. Liu[35], Fang Liu[1], Feng Liu[6], H. B. Liu[12], H. H. Liu[1], H. H. Liu[16], H. M. Liu[1], J. Liu[1], J. B. Liu[46,a], J. P. Liu[51], J. Y. Liu[1], K. Liu[39], K. Y. Liu[27], L. D. Liu[31], P. L. Liu[1,a], Q. Liu[41], S. B. Liu[46,a], X. Liu[26], Y. B. Liu[30], Y. Y. Liu[30], Z. A. Liu[1,a], Zhiqing Liu[22], H. Loehner[25], X. C. Lou[1,a,g], H. J. Lu[17], J. G. Lu[1,a], Y. Lu[1], Y. P. Lu[1,a], C. L. Luo[28], M. X. Luo[52], T. Luo[42], X. L. Luo[1,a], X. R. Lyu[41], F. C. Ma[27], H. L. Ma[1], L. L. Ma[33], M. M. Ma[1], Q. M. Ma[1], T. Ma[1], X. N. Ma[30], X. Y. Ma[1,a], Y. M. Ma[33], F. E. Maas[14], M. Maggiora[49A,49C], Q. A. Malik[48], Y. J. Mao[31], Z. P. Mao[1], S. Marcello[49A,49C], J. G. Messchendorp[25], G. Mezzadri[21B], J. Min[1,a], T. J. Min[1], R. E. Mitchell[19], X. H. Mo[1,a], Y. J. Mo[6], C. Morales Morales[14], N. Yu. Muchnoi[9,e], H. Muramatsu[43], P. Musiol[4], Y. Nefedov[23], F. Nerling[10], I. B. Nikolaev[9,e], Z. Ning[1,a], S. Nisar[8], S. L. Niu[1,a], X. Y. Niu[1], S. L. Olsen[32], Q. Ouyang[1,a], S. Pacetti[20B], Y. Pan[46,a], P. Patteri[20A], M. Pelizaeus[4], H. P. Peng[46,a], K. Peters[10,i], J. Pettersson[50], J. L. Ping[28], R. G. Ping[1], R. Poling[43], V. Prasad[1], H. R. Qi[2], M. Qi[29], S. Qian[1,a], C. F. Qiao[41], L. Q. Qin[33], N. Qin[51], X. S. Qin[1], Z. H. Qin[1,a], J. F. Qiu[1], K. H. Rashid[48], C. F. Redmer[22], M. Ripka[22], G. Rong[1], Ch. Rosner[14], X. D. Ruan[12], A. Sarantsev[23,f], M. Savrié[21B], C. Schnier[4], K. Schoenning[50], W. Shan[31], M. Shao[46,a], C. P. Shen[2], P. X. Shen[30], X. Y. Shen[1], H. Y. Sheng[1], W. M. Song[1], X. Y. Song[1], S. Sosio[49A,49C], S. Spataro[49A,49C], G. X. Sun[1], J. F. Sun[15], S. S. Sun[1], X. H. Sun[1], Y. J. Sun[46,a], Y. Z. Sun[1], Z. J. Sun[1,a], Z. T. Sun[19], C. J. Tang[36], X. Tang[1], I. Tapan[40C], E. H. Thorndike[44], M. Tiemens[25], I. Uman[40D], G. S. Varner[42], B. Wang[30], B. L. Wang[41], D. Wang[31], D. Y. Wang[31], K. Wang[1,a], L. L. Wang[1], L. S. Wang[1], M. Wang[33], P. Wang[1], P. L. Wang[1], W. Wang[1,a], W. P. Wang[46,a], X. F. Wang[39], Y. Wang[37], Y. D. Wang[14], Y. F. Wang[1,a], Y. Q. Wang[22], Z. Wang[1,a], Z. G. Wang[1,a], Z. H. Wang[46,a], Z. Y. Wang[1], Z. Y. Wang[1], T. Weber[22], D. H. Wei[11], P. Weidenkaff[22], S. P. Wen[1], U. Wiedner[4], M. Wolke[50], L. H. Wu[1], L. J. Wu[1], Z. Wu[1,a], L. Xia[46,a], L. G. Xia[39], Y. Xia[18], D. Xiao[1], H. Xiao[47], Z. J. Xiao[28], Y. G. Xie[1,a], Yuehong Xie[6], Q. L. Xiu[1,a], G. F. Xu[1], J. J. Xu[1], L. Xu[1], Q. J. Xu[13], Q. N. Xu[41], X. P. Xu[37], L. Yan[49A,49C], W. B. Yan[46,a], W. C. Yan[46,a], Y. H. Yan[18], H. J. Yang[34,j], H. X. Yang[1], L. Yang[51], Y. X. Yang[11], M. Ye[1,a], M. H. Ye[7], J. H. Yin[1], Z. Y. You[38], B. X. Yu[1,a], C. X. Yu[30], J. S. Yu[26], C. Z. Yuan[1], Y. Yuan[1], A. Yuncu[40B,b], A. A. Zafar[48], Y. Zeng[18], Z. Zeng[46,a], B. X. Zhang[1], B. Y. Zhang[1,a], C. C. Zhang[1], D. H. Zhang[1], H. H. Zhang[38], H. Y. Zhang[1,a], J. Zhang[1], J. J. Zhang[1], J. L. Zhang[1], J. Q. Zhang[1], J. W. Zhang[1,a], J. Y. Zhang[1], J. Z. Zhang[1], K. Zhang[1], L. Zhang[1], S. Q. Zhang[30], X. Y. Zhang[33], Y. Zhang[1], Y. Zhang[1], Y. H. Zhang[1,a], Y. N. Zhang[41], Y. T. Zhang[46,a], Yu Zhang[41], Z. H. Zhang[6], Z. P. Zhang[46], Z. Y. Zhang[51], G. Zhao[1], J. W. Zhao[1,a], J. Y. Zhao[1], J. Z. Zhao[1,a], Lei Zhao[46,a], Ling Zhao[1], M. G. Zhao[30], Q. Zhao[1], Q. W. Zhao[1], S. J. Zhao[53], T. C. Zhao[1], Y. B. Zhao[1,a], Z. G. Zhao[46,a], A. Zhemchugov[23,c], B. Zheng[47], J. P. Zheng[1,a], W. J. Zheng[33], Y. H. Zheng[41], B. Zhong[28], L. Zhou[1,a], X. Zhou[51], X. K. Zhou[46,a], X. R. Zhou[46,a], X. Y. Zhou[1], K. Zhu[1], K. J. Zhu[1,a], S. Zhu[1], S. H. Zhu[45], X. L. Zhu[39], Y. C. Zhu[46,a], Y. S. Zhu[1], Z. A. Zhu[1], J. Zhuang[1,a], L. Zotti[49A,49C], B. S. Zou[1], J. H. Zou[1]

(BESIII Collaboration)

[1] *Institute of High Energy Physics, Beijing 100049, People's Republic of China*

[2] Beihang University, Beijing 100191, People's Republic of China
[3] Beijing Institute of Petrochemical Technology, Beijing 102617, People's Republic of China
[4] Bochum Ruhr-University, D-44780 Bochum, Germany
[5] Carnegie Mellon University, Pittsburgh, Pennsylvania 15213, USA
[6] Central China Normal University, Wuhan 430079, People's Republic of China
[7] China Center of Advanced Science and Technology, Beijing 100190, People's Republic of China
[8] COMSATS Institute of Information Technology, Lahore, Defence Road, Off Raiwind Road, 54000 Lahore, Pakistan
[9] G.I. Budker Institute of Nuclear Physics SB RAS (BINP), Novosibirsk 630090, Russia
[10] GSI Helmholtzcentre for Heavy Ion Research GmbH, D-64291 Darmstadt, Germany
[11] Guangxi Normal University, Guilin 541004, People's Republic of China
[12] Guangxi University, Nanning 530004, People's Republic of China
[13] Hangzhou Normal University, Hangzhou 310036, People's Republic of China
[14] Helmholtz Institute Mainz, Johann-Joachim-Becher-Weg 45, D-55099 Mainz, Germany
[15] Henan Normal University, Xinxiang 453007, People's Republic of China
[16] Henan University of Science and Technology, Luoyang 471003, People's Republic of China
[17] Huangshan College, Huangshan 245000, People's Republic of China
[18] Hunan University, Changsha 410082, People's Republic of China
[19] Indiana University, Bloomington, Indiana 47405, USA
[20] (A)INFN Laboratori Nazionali di Frascati, I-00044, Frascati, Italy; (B)INFN and University of Perugia, I-06100, Perugia, Italy
[21] (A)INFN Sezione di Ferrara, I-44122, Ferrara, Italy; (B)University of Ferrara, I-44122, Ferrara, Italy
[22] Johannes Gutenberg University of Mainz, Johann-Joachim-Becher-Weg 45, D-55099 Mainz, Germany
[23] Joint Institute for Nuclear Research, 141980 Dubna, Moscow region, Russia
[24] Justus-Liebig-Universitaet Giessen, II. Physikalisches Institut, Heinrich-Buff-Ring 16, D-35392 Giessen, Germany
[25] KVI-CART, University of Groningen, NL-9747 AA Groningen, The Netherlands
[26] Lanzhou University, Lanzhou 730000, People's Republic of China
[27] Liaoning University, Shenyang 110036, People's Republic of China
[28] Nanjing Normal University, Nanjing 210023, People's Republic of China
[29] Nanjing University, Nanjing 210093, People's Republic of China
[30] Nankai University, Tianjin 300071, People's Republic of China
[31] Peking University, Beijing 100871, People's Republic of China
[32] Seoul National University, Seoul, 151-747 Korea
[33] Shandong University, Jinan 250100, People's Republic of China
[34] Shanghai Jiao Tong University, Shanghai 200240, People's Republic of China
[35] Shanxi University, Taiyuan 030006, People's Republic of China
[36] Sichuan University, Chengdu 610064, People's Republic of China
[37] Soochow University, Suzhou 215006, People's Republic of China
[38] Sun Yat-Sen University, Guangzhou 510275, People's Republic of China
[39] Tsinghua University, Beijing 100084, People's Republic of China
[40] (A)Ankara University, 06100 Tandogan, Ankara, Turkey; (B)Istanbul Bilgi University, 34060 Eyup, Istanbul, Turkey; (C)Uludag University, 16059 Bursa, Turkey; (D)Near East University, Nicosia, North Cyprus, Mersin 10, Turkey
[41] University of Chinese Academy of Sciences, Beijing 100049, People's Republic of China
[42] University of Hawaii, Honolulu, Hawaii 96822, USA
[43] University of Minnesota, Minneapolis, Minnesota 55455, USA
[44] University of Rochester, Rochester, New York 14627, USA
[45] University of Science and Technology Liaoning, Anshan 114051, People's Republic of China
[46] University of Science and Technology of China, Hefei 230026, People's Republic of China
[47] University of South China, Hengyang 421001, People's Republic of China
[48] University of the Punjab, Lahore-54590, Pakistan
[49] (A)University of Turin, I-10125, Turin, Italy; (B)University of Eastern Piedmont, I-15121, Alessandria, Italy; (C)INFN, I-10125, Turin, Italy

[50] Uppsala University, Box 516, SE-75120 Uppsala, Sweden
[51] Wuhan University, Wuhan 430072, People's Republic of China
[52] Zhejiang University, Hangzhou 310027, People's Republic of China
[53] Zhengzhou University, Zhengzhou 450001, People's Republic of China

[a] Also at State Key Laboratory of Particle Detection and Electronics, Beijing 100049, Hefei 230026, People's Republic of China
[b] Also at Bogazici University, 34342 Istanbul, Turkey
[c] Also at the Moscow Institute of Physics and Technology, Moscow 141700, Russia
[d] Also at the Functional Electronics Laboratory, Tomsk State University, Tomsk, 634050, Russia
[e] Also at the Novosibirsk State University, Novosibirsk, 630090, Russia
[f] Also at the NRC "Kurchatov Institute, PNPI, 188300, Gatchina, Russia
[g] Also at University of Texas at Dallas, Richardson, Texas 75083, USA
[h] Also at Istanbul Arel University, 34295 Istanbul, Turkey
[i] Also at Goethe University Frankfurt, 60323 Frankfurt am Main, Germany
[j] Also at Institute of Nuclear and Particle Physics, Shanghai Key Laboratory for Particle Physics and Cosmology, Shanghai 200240, People's Republic of China

The cross sections of $e^+e^- \to \pi^+\pi^- h_c$ at center-of-mass energies from 3.896 to 4.600 GeV are measured using data samples collected with the BESIII detector operating at the Beijing Electron Positron Collider. The cross sections are found to be of the same order of magnitude as those of $e^+e^- \to \pi^+\pi^- J/\psi$ and $e^+e^- \to \pi^+\pi^-\psi(2S)$, but the line shape is inconsistent with the Y states observed in the latter two modes. Two structures are observed in the $e^+e^- \to \pi^+\pi^- h_c$ cross sections around 4.22 and 4.39 GeV/c^2, which we call $Y(4220)$ and $Y(4390)$, respectively. A fit with a coherent sum of two Breit-Wigner functions results in a mass of $(4218.4 \pm 4.0 \pm 0.9)$ MeV/c^2 and a width of $(66.0 \pm 9.0 \pm 0.4)$ MeV for the $Y(4220)$, and a mass of $(4391.6 \pm 6.3 \pm 1.0)$ MeV/c^2 and a width of $(139.5 \pm 16.1 \pm 0.6)$ MeV for the $Y(4390)$, where the first uncertainties are statistical and the second ones systematic.

PACS numbers: 14.40.Rt, 14.40.Pq, 13.66.Bc, 13.25.Gv

In the last decade, a series of charmonium-like states have been observed at e^+e^- colliders. These states challenge the understanding of charmonium spectroscopy as well as QCD calculations [1, 2]. According to potential models, there are five vector charmonium states between the $D\bar{D}$ mass threshold and 4.7 GeV/c^2, namely the $3S$, $2D$, $4S$, $3D$, and $5S$ states [1]. From experimental studies, besides the three well established structures observed in the inclusive hadronic cross section [3], $i.e.$, $\psi(4040)$, $\psi(4160)$, and $\psi(4415)$, five Y states, $i.e.$, $Y(4008)$, $Y(4230)$, $Y(4260)$, $Y(4360)$, and $Y(4660)$ have been reported in initial state radiation (ISR) processes $e^+e^- \to \gamma_{\rm ISR}\pi^+\pi^- J/\psi$ or $e^+e^- \to \gamma_{\rm ISR}\pi^+\pi^-\psi(2S)$ at the B-factories [4–11] or in the direct production processes at the CLEO and BESIII experiments [12, 13] The overpopulation of structures in this region and mismatch of the properties between the potential model prediction and experimental measurements make them good candidates for exotic states. Various scenarios have been proposed, which interpret one or some of them as hybrid states, tetraquark states, or molecular states [14].

The study of charmonium-like states in different production processes supplies useful information on their properties. The process $e^+e^- \to \pi^+\pi^- h_c$ was first studied by CLEO [15] at center-of-mass (CM) energies $\sqrt{s}$ from 4.000 to 4.260 GeV. A 10σ signal at 4.170 GeV and a hint of a rising cross section at 4.260 GeV were observed. Using data samples taken at 13 CM energies from 3.900 to 4.420 GeV [16], BESIII reported the measurement of the cross section of $e^+e^- \to \pi^+\pi^- h_c$ [17]. Unlike the line shape of the process $e^+e^- \to \pi^+\pi^- J/\psi$, there is a broad structure in the high energy region with a possible local maximum at around 4.23 GeV in $e^+e^- \to \pi^+\pi^- h_c$. Based on the CLEO measurement at $\sqrt{s} = 4.170$ GeV and the BESIII measurement, two assumptions were made to describe the cross section in Ref. [18]. In both assumptions, a narrow structure exists at around 4.23 GeV, while the situation in the high energy region is unclear due to the lack of experimental data.

In this Letter, we present a follow-up study of $e^+e^- \to \pi^+\pi^- h_c$ at CM energies from 3.896 to 4.600 GeV using data samples taken at 79 energy points [19] with the BESIII detector [20]. Two resonant structures are observed at $\sqrt{s} = 4.22$ and 4.39 GeV (hereafter referred to as $Y(4220)$ and $Y(4390)$). The integrated luminosity at each energy point is measured with an uncertainty of 1.0% using large-angle Bhabha events [21, 22]. There are 17 energy points where the integrated luminosities are larger than 40 pb^{-1} (referred to as 'XYZ data sample' hereafter), while the integrated luminosities for the other energy points are smaller than 20 pb^{-1} (referred to as 'R-scan data sample' hereafter). The CM energies for the XYZ data sample are measured with $e^+e^- \to \gamma_{\rm ISR/FSR}\mu^+\mu^-$ events with an uncertainty of ± 0.8 MeV [23], which is dominated by the systematic uncertainty. A similar method is used for the R-scan data sample with multihadron final states [24]. In this study, the h_c is reconstructed via its electric-dipole transition $h_c \to \gamma\eta_c$ with $\eta_c \to X_i$, where X_i is one of 16 exclusive hadronic final states: $p\bar{p}$, $2(\pi^+\pi^-)$, $2(K^+K^-)$, $\pi^+\pi^-K^+K^-$, $\pi^+\pi^-p\bar{p}$, $3(\pi^+\pi^-)$, $2(\pi^+\pi^-)K^+K^-$, $K_S^0K^\pm\pi^\mp$, $K_S^0K^\pm\pi^\mp\pi^+\pi^-$, $K^+K^-\pi^0$, $p\bar{p}\pi^0$, $K^+K^-\eta$, $\pi^+\pi^-\eta$, $2(\pi^+\pi^-)\eta$, $\pi^+\pi^-\pi^0\pi^0$, and $2(\pi^+\pi^-\pi^0)$. Here, the K_S^0 is reconstructed using its decay to $\pi^+\pi^-$, and the π^0 and η from the $\gamma\gamma$ final state.

Monte Carlo (MC) simulated events are used to optimize the selection criteria, determine the detection efficiency, and estimate the possible backgrounds. The simulation of the BESIII detector is based on GEANT4 [25] and includes the geometric description of the BESIII detector and the detector response. For the signal process, we use a sample of $e^+e^- \to \pi^+\pi^-h_c$ MC events generated according to phase space. ISR is simulated with KKMC [26] with a maximum energy for the ISR photon corresponding to the $\pi^+\pi^-h_c$ mass threshold.

We select signal candidates with the same method as that described in Ref. [17]. Figure 1 shows the scatter plot of the invariant mass of the η_c candidate versus the one of the h_c candidate for the data sample at $\sqrt{s} = 4.416$ GeV, as well as the invariant mass distribution of $\gamma\eta_c$ in the η_c signal region. A clear $h_c \to \gamma\eta_c$ signal is observed. The η_c signal region is defined by a mass window around the nominal η_c mass [3], which is ± 50 MeV/c^2 with efficiency about 84% (± 45 MeV/c^2 with efficiency about 80%) from MC simulation for final states with only charged or K_S^0 particles (for those including π^0 or η).

We determine the number of $\pi^+\pi^-h_c$ signal events ($n_{h_c}^{\rm obs}$) from the $\gamma\eta_c$ invariant mass distribution. For the XYZ data sample, the $\gamma\eta_c$ mass spectrum is fitted with the MC simulated signal shape convolved with a Gaussian function to reflect the mass resolution difference between the data and MC simulation, together with a linear background. The fit to the data sample at $\sqrt{s} = 4.416$ GeV is shown in Fig. 1 (right). The tail on the high mass side is due to events with ISR; this is simulated with KKMC in MC, and its fraction is fixed in the fit. For the data samples with large statistics ($\sqrt{s} = 4.226$, 4.258, 4.358, and 4.416 GeV), the fit is applied to the 16 η_c decay modes simultaneously with the number of signal events in each decay mode constrained by the corresponding branching fraction [27]. For the data samples at the other energy points, we fit the mass spectrum summed over all η_c decay modes. For the R-scan data sample, the number of signal events is calculated by counting the entries in the h_c signal region [3.515, 3.535] GeV/c^2 ($n^{\rm sig}$) and the entries in the h_c sideband regions [3.475, 3.495] GeV/c^2 and [3.555, 3.575] GeV/c^2 ($n^{\rm side}$) using the formula $n_{h_c}^{\rm obs} = n^{\rm sig} - f\cdot n^{\rm side}$. Here, the scale factor $f = 0.5$ is the ratio of the size of the signal region and the background region, and the background is assumed to be distributed linearly in the region of interest.

The Born cross section is calculated from

$$\sigma^{\rm B} = \frac{n_{h_c}^{\rm obs}}{\mathcal{L}(1+\delta)|1+\Pi|^2\sum_{i=1}^{16}\epsilon_i\mathcal{B}(\eta_c\to X_i)\mathcal{B}(h_c\to\gamma\eta_c)},$$

where $n_{h_c}^{\rm obs}$ is the number of observed signal events, $\mathcal{L}$ is the integrated luminosity, $(1+\delta)$ is the ISR correction factor obtained using the QED calculation as described in Ref. [28] and taking the formula used to fit the cross section measured in this analysis after two iterations as input, $|1+\Pi|^2$ is the correction factor for vacuum polarization [29], ϵ_i and $\mathcal{B}(\eta_c \to X_i)$ are the detection efficiency and branching fraction for the i-th η_c decay mode [27], $\mathcal{B}(h_c \to \gamma\eta_c)$ is the branching fraction of $h_c \to \gamma\eta_c$ [3]. The Born cross sections are shown in Fig. 2 with dots and squares for R-scan and XYZ data sample, respectively, and the results are summarised in the supplemental material [19] together with all numbers used in the calculation of the Born cross sections.

Systematic uncertainties in the cross section measurement mainly come from the luminosity measurement, the branching fraction of $h_c \to \gamma\eta_c$ and $\eta_c \to X_i$, the detection efficiency, the ISR correction factor, and the fit. The uncertainty due to the vacuum polarization is negligible. The uncertainty in the integrated luminosity is 1% at each energy point. The uncertainty sources for the detection efficiency include systematic uncertainties in tracking efficiency (1% per track), photon reconstruction (1% per photon), and K_S^0 reconstruction (1.2% per K_S^0). Further uncertainties arise from the π^0/η mass window requirement (1% per π^0/η), the $\chi^2_{\rm 4C}$ requirement, η_c parameters and line shape, possible intermediate states in the $\pi^\pm h_c$ and $\pi^+\pi^-$ mass spectra, and the limited statistics of the MC simulation.

The uncertainty due to the $\chi^2_{\rm 4C}$ requirement is estimated by correcting the helix parameters of the simulated charged tracks to match the resolution found in data, and repeating the analysis [30]. Uncertainties due to the η_c parameters and line shape are estimated by varying them in the MC simulation. When producing MC $e^+e^- \to \pi^+\pi^-h_c$ events through the intermediate states $Z_c(3900)$ or $Z_c(4020)$, the parameters of the $Z_c(3900)$ and $Z_c(4020)$ are fixed to the average values from the published measurements [11, 17, 31–33]. The quantum numbers of both $Z_c(3900)$ and $Z_c(4020)$ are assumed to be $J^P = 1^+$. The differences in the efficiency obtained from phase space MC samples and those with intermediate Z_c states are taken as the uncertainties from possible intermediate states in the $\pi^\pm h_c$ system. The uncertainty from intermediate states in the $\pi^+\pi^-$ system is estimated by re-weighting the $\pi^+\pi^-$ mass distribution in the phase space MC sample according to the data, and the resulting difference in the efficiency is considered as uncertainty. The uncertainties due to data/MC differences in the detection efficiency are determined to be between 5.5% and 10.8%, depending on the η_c decay modes and the CM energy. Combining the uncertainties for the branching fractions of η_c decays [27], the uncertainties for the average efficiency $\sum_{i=1}^{16}\epsilon_i\mathcal{B}(\eta_c \to X_i)$ are between 6.4% and 9.1% depending on the CM energy.

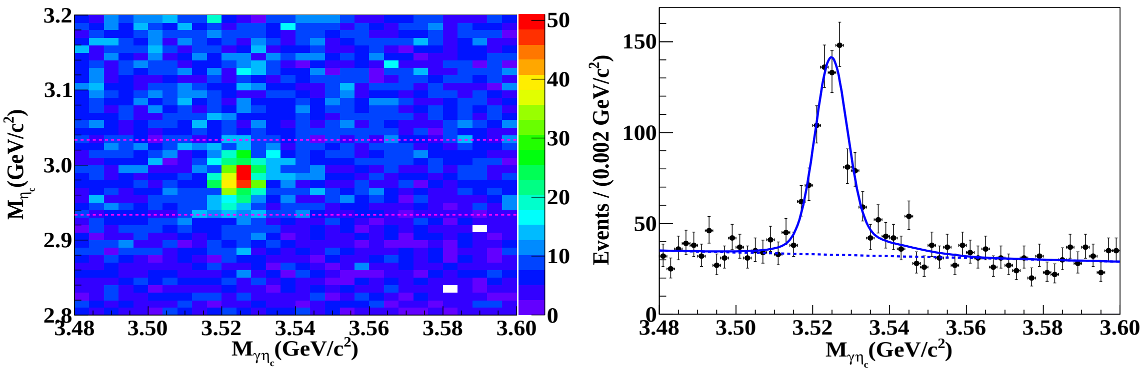

FIG. 1. (*left panel*) Scatter plot of the mass of the η_c candidate M_{η_c} versus the mass of the h_c candidate $M_{\gamma\eta_c}$. (*right panel*) Distribution of $M_{\gamma\eta_c}$ for events in the η_c signal region. Points with error bars show the data at $\sqrt{s} = 4.416$ GeV and the curves are the best fit described in the text.

The uncertainty in the ISR correction is estimated as described in Ref. [31]. Uncertainties due to the choice of the signal shape, the background shape, the mass resolution, and fit range are estimated by changing the h_c and η_c resonant parameters and line shapes in the MC simulation, changing the background function from a linear to a second-order polynomial, changing the mass resolution difference between the data and the MC simulation by one standard deviation, and by extending or shrinking the fit range.

Assuming all of the sources are independent, the total systematic uncertainty in the $\pi^+\pi^-h_c$ cross section measurement is determined to be 9.4%–13.6% depending on the CM energy. The uncertainty in $\mathcal{B}(h_c \to \gamma\eta_c)$ is 11.8% [3], common to all energy points, and quoted separately in the cross section measurement. Altogether, about 95% of the total systematic errors are common to all the energy points.

A maximum likelihood method is used to fit the dressed cross sections (with vacuum polarization effects) to determine the parameters of the resonant structures. The likelihood is constructed taking the fluctuations of the number of signal and background events into account (the definition is described in the supplemental material [19]). Assuming that the $\pi^+\pi^-h_c$ signal comes from two resonances, the cross section is parameterized as the coherent sum of two constant width relativistic Breit-Wigner functions, *i.e.*,

$$\sigma(m) = |\mathrm{B}_1(m) \cdot \sqrt{\frac{P(m)}{P(M_1)}} + e^{i\phi}\mathrm{B}_2(m) \cdot \sqrt{\frac{P(m)}{P(M_2)}}|^2,$$

where $\mathrm{B}_j(m) = \frac{\sqrt{12\pi\Gamma_j^{el}\Gamma_j}}{m^2 - M_j^2 + iM_j\Gamma_j}$ with $j = 1$ or 2 is the Breit-Wigner function, and $P(m)$ is the 3-body phase space factor. The masses M_j, the total widths Γ_j, the products of the electronic partial width and the branching fraction to $\pi^+\pi^-h_c$ $\Gamma_j^{el} = (\Gamma_{e^+e^-}\mathcal{B}(\pi^+\pi^-h_c))_j$, and the relative phase ϕ between the two Breit-Wigner functions are free parameters in the fit. Only the statistical uncertainty is considered in the fit. There are two solutions from the fit, one of them is shown in Fig. 2. The second solution is very close to the one shown here. This can been proved analytically as derived in Ref. [34], which relates the two solutions from the fit when a sum of two coherent Breit-Wigner functions is used. The parameters determined from the fit are $M_1 = (4218.4 \pm 4.0)$ MeV$/c^2$, $\Gamma_1 = (66.0 \pm 9.0)$ MeV, and $\Gamma_1^{el} = (4.6 \pm 4.1)$ eV for $Y(4220)$, $M_2 = (4391.6 \pm 6.3)$ MeV$/c^2$, $\Gamma_2 = (139.5 \pm 16.1)$ MeV, and $\Gamma_2^{el} = (11.8 \pm 9.7)$ eV for $Y(4390)$. The relative phase ϕ is (3.1 ± 1.5) rad. The correlation matrix of the fit parameters shows large correlation between the Γ_j^{el} and ϕ (see supplemental material [19]).

Fitting the dressed cross section with only one resonance yields a worse result, the change of the likelihood value from two resonances to one resonance is $[\Delta(-2\ln L) = 113.5]$. Taking the change in the number of degrees of freedom (4) into account, the significance for the assumption of two resonant structures over the assumption of one resonant structure is 10σ. We also fit the cross section with the coherent sum of three Breit-Wigner functions, or the coherent sum of two Breit-Wigner functions and a phase space term. Both assumptions improve the fit quality, but the significances of the third resonance and the phase space term are only 2.6σ and 2.9σ, respectively.

The systematic uncertainties in the resonance parameters mainly come from the absolute CM energy measurement, the CM energy spread, and the systematic uncertainty on the cross section measurement. The uncertainty from the CM energy measurement includes the uncertainty of the CM energy and the assumption made in the measurement for R-scan data sample. Due to the low statistics at each energy point in the R-scan data sample, we approximate the difference between the requested and the actual center-of-mass energy by a common constant. To assess the systematic uncertainty connected with this assumption, we replace the constant by a CM energy-dependent second-order polynomial. The systematic uncertainty of the CM energy is common for all the energy points

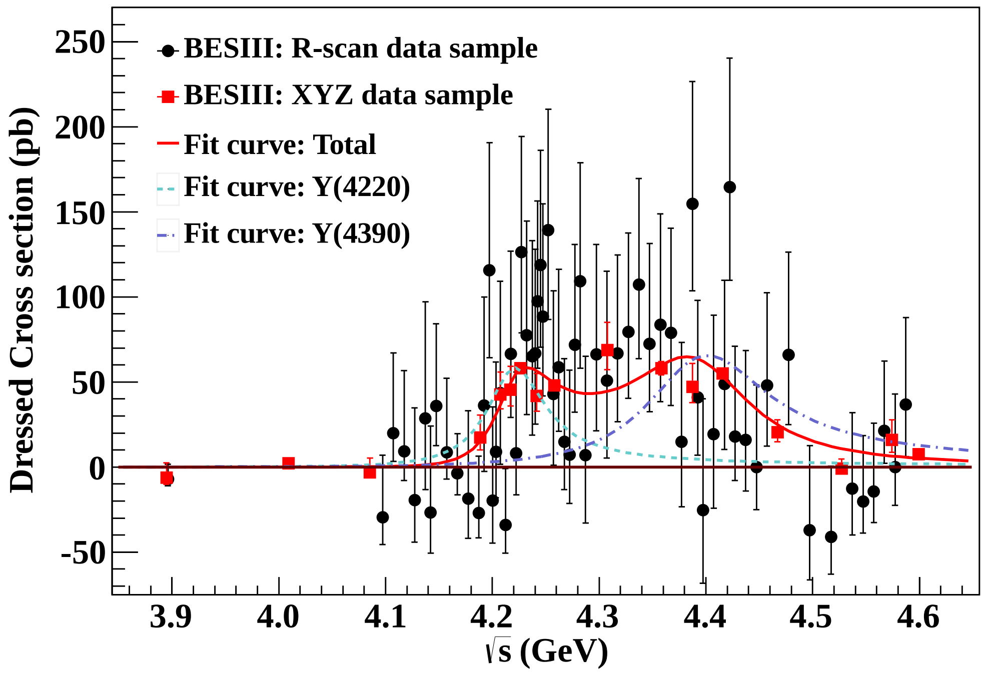

FIG. 2. Fit to the dressed cross section of $e^+e^- \to \pi^+\pi^-h_c$ with the coherent sum of two Breit-Wigner functions (solid curve). The dash (dash-dot) curve shows the contribution from the two structures $Y(4220)$ ($Y(4390)$). The dots with error bars are the cross sections for R-scan data sample, the squares with error bars are the cross sections for XYZ data sample. Here the error bars are statistical uncertainty only.

and will propagate to the mass measurement (0.8 MeV). The changes on the parameters are taken as uncertainty. The uncertainty from CM energy spread is estimated by convoluting the fit formula with a Gaussian function with a width of 1.6 MeV, which is beam spread, measured by the Beam Energy Measurement System [35]. The uncertainty from the cross section measurement is divided into two parts. The first one is uncorrelated among the different CM energy points and comes mainly from the fit to the $\gamma\eta_c$ invariant mass spectrum to determine the signal yields. The corresponding uncertainty is estimated by including the uncertainty in the fit to the cross section, and taking the differences on the parameters as uncertainties. The second part includes all the other sources, is common for all data points (14.8%), and only affects the Γ^{el} measurement. Table I summarizes the systematic uncertainty in the resonance parameters.

In summary, we measure the $e^+e^- \to \pi^+\pi^-h_c$ Born cross section using data at 79 CM energy points from 3.896 to 4.600 GeV. The cross sections are of the same order of magnitude as those of the $e^+e^- \to \pi^+\pi^-J/\psi$ and $e^+e^- \to \pi^+\pi^-\psi(2S)$ [4–12], but with a different line shape. The cross section drops in the high energy region, but more slowly than for the $e^+e^- \to \pi^+\pi^-J/\psi$ process. Assuming the $\pi^+\pi^-h_c$ events come from two resonances, we obtain $M = (4218.4 \pm 4.0 \pm 0.9)$ MeV/c^2, $\Gamma = (66.0 \pm 9.0 \pm 0.4)$ MeV, and $\Gamma^{el} = (4.6 \pm 4.1 \pm 0.8)$ eV for $Y(4220)$, and $M = (4391.6 \pm 6.3 \pm 1.0)$ MeV/c^2, $\Gamma = (139.5 \pm 16.1 \pm 0.6)$ MeV, and $\Gamma^{el} = (11.8 \pm 9.7 \pm 1.9)$ eV for $Y(4390)$, with a relative phase of $\phi = (3.1 \pm 1.5 \pm 0.2)$ rad. The parameters of these structures are different from those of $Y(4260)$, $Y(4360)$, and $\psi(4415)$ [3]. The resonance parameters of $Y(4220)$ are consistent with those of the resonance observed in $e^+e^- \to \omega\chi_{c0}$ [13].

The two resonances observed in $e^+e^- \to \pi^+\pi^-h_c$ process are located in the mass region between 4.2 and 4.4 GeV/c^2, where the vector charmonium hybrid states are predicted from various QCD calculations [36, 37]. The mass of $Y(4220)$ is lower than that of $Y(4260)$ observed in the $e^+e^- \to \pi^+\pi^-J/\psi$ process. The smaller mass is consistent with some of the theoretical calculations for the mass of $Y(4260)$ when explaining it as a $D_1\bar{D}$ molecule [38, 39].

The BESIII collaboration thanks the staff of BEPCII and the IHEP computing center for their strong support. This work is supported in part by National Key Basic Research Program of China under Contract No. 2015CB856700; National Natural Science Foundation of China (NSFC) under Contracts Nos. 11235011, 11322544, 11335008, 11425524; the Chinese Academy of Sciences (CAS) Large-Scale Scientific Facility Program; the CAS Center for Excellence in Particle Physics (CCEPP); the Collaborative Innovation Center for Particles and Interactions (CICPI); Joint Large-Scale Scientific Facility Funds of the NSFC and CAS under Con-

TABLE I. The systematic uncertainty in the measurement of the resonance parameters, where $\Gamma^{el} = \Gamma_{e^+e^-}\mathcal{B}(\pi^+\pi^- h_c)$ is the product of the electronic partial width and the branching fraction to $\pi^+\pi^- h_c$. CM energy[1] represents the uncertainty from the systematic uncertainty of CM energy measurement and CM energy[2] is the uncertainty from assumption made in the measurement of CM energy for R-scan data sample. Cross section[1(2)] represents the uncertainty from the systematic uncertainties of the cross section measurement which are un-correlated (common) in each energy point.

Sources	$Y(4220)$			$Y(4390)$			ϕ (rad)
	M (MeV/c^2)	Γ (MeV)	Γ^{el} (eV)	M (MeV/c^2)	Γ (MeV)	Γ^{el} (eV)	
CM energy[1(2)]	0.8(0.1)	$-$(0.1)	$-$(0.2)	0.8(0.1)	$-$(0.2)	$-$(0.3)	$-$(0.1)
CM energy spread	0.1	0.3	0.3	0.1	0.1	0.7	0.1
Cross section[1(2)]	0.1($-$)	$-$($-$)	0.2(0.7)	0.6($-$)	0.5($-$)	0.4(1.7)	0.1($-$)
Total	0.9	0.4	0.8	1.0	0.6	1.9	0.2

tracts Nos. U1232201, U1332201; CAS under Contracts Nos. KJCX2-YW-N29, KJCX2-YW-N45; 100 Talents Program of CAS; National 1000 Talents Program of China; INPAC and Shanghai Key Laboratory for Particle Physics and Cosmology; German Research Foundation DFG under Contracts Nos. Collaborative Research Center CRC 1044, FOR 2359; Istituto Nazionale di Fisica Nucleare, Italy; Joint Large-Scale Scientific Facility Funds of the NSFC and CAS under Contract No. U1532257; Joint Large-Scale Scientific Facility Funds of the NSFC and CAS under Contract No. U1532258; Koninklijke Nederlandse Akademie van Wetenschappen (KNAW) under Contract No. 530-4CDP03; Ministry of Development of Turkey under Contract No. DPT2006K-120470; NSFC under Contract No. 11275266; The Swedish Resarch Council; U. S. Department of Energy under Contracts Nos. DE-FG02-05ER41374, DE-SC-0010504, de-sc0012069, DESC0010118; U.S. National Science Foundation; University of Groningen (RuG) and the Helmholtzzentrum fuer Schwerionenforschung GmbH (GSI), Darmstadt; WCU Program of National Research Foundation of Korea under Contract No. R32-2008-000-10155-0.

[1] For a recent review, see N. Brambilla *et al.*, Eur. Phys. J. C **71**, 1534 (2011).
[2] R. A. Briceno *et al.*, Chin. Phys. C **40(4)**, 042001 (2016).
[3] K. A. Olive *et al.* (Particle Data Group), Chin. Phys. C **38(9)**, 090001 (2014).
[4] B. Aubert *et al.* (BaBar Collaboration), Phys. Rev. Lett. **95**, 142001 (2005).
[5] C. Z. Yuan *et al.* (Belle Collaboration), Phys. Rev. Lett. **99**, 182004 (2007).
[6] B. Aubert *et al.* (BaBar Collaboration), Phys. Rev. Lett. **98**, 212001 (2007).
[7] X. L. Wang *et al.* (Belle Collaboration), Phys. Rev. Lett. **99**, 142002 (2007).
[8] J. P. Lees *et al.* (BaBar Collaboration), Phys. Rev. D **89**, 111103 (2014).
[9] X. L. Wang *et al.* (Belle Collaboration), Phys. Rev. D **91**, 112007 (2015).
[10] J. P. Lees *et al.* (BaBar Collaboration), Phys. Rev. D **86**, 051102(R) (2012).
[11] Z. Q. Liu *et al.* (Belle Collaboration), Phys. Rev. Lett. **110**, 252002 (2013).
[12] T. E. Coan *et al.* (CLEO Collaboration), Phys. Rev. Lett. **96**, 162003 (2006).
[13] M. Ablikim *et al.* (BESIII Collaboration), Phys. Rev. Lett. **114**, 092003 (2015).
[14] H. X. Chen, W. Chen, X. Liu, and S. L. Zhu, Phys. Rep. **639**, 1 (2016).
[15] T. K. Pedlar *et al.* (CLEO Collaboration), Phys. Rev. Lett. **107**, 041803 (2011).
[16] The data samples are the same as those used in this study except at 4.420 GeV. At 4.420 GeV, more data has been collected and analysed. Besides, the CM energies at all energy points have been remeasured using $e^+e^- \to \gamma_{\rm ISR/FSR}\mu^+\mu^-$ events, and found to be a few MeV smaller.
[17] M. Ablikim *et al.* (BESIII Collaboration), Phys. Rev. Lett. **111**, 242001 (2013).
[18] C. Z. Yuan, Chin. Phys. C **38(4)**, 043001 (2014).
[19] See supplemental material at [URL will be inserted by publisher] for a summary of number of signal events, luminosity, and Born cross section at each energy point, the definition of the likelihood used in the fit to the dressed cross section, and the correlation matrix of the fit parameters from the fit.
[20] M. Ablikim *et al.* (BESIII Collaboration), Nucl. Instrum. Meth. A **614**, 345 (2010).
[21] M. Ablikim *et al.* (BESIII Collaboration), Chin. Phys. C **39(9)**, 093001 (2015).
[22] M. Ablikim *et al.* (BESIII Collaboration), “Measurement of the integrated luminosities for R scan experiment at BESIII”, paper in preparation.
[23] M. Ablikim *et al.* (BESIII Collaboration), Chin. Phys. C **40(6)**, 063001 (2016).
[24] M. Ablikim *et al.* (BESIII Collaboration), “Measurement of the center-of-mass energies for R scan experiment”, paper in preparation.
[25] S. Agostinelli *et al.* (GEANT4 Collaboration), Nucl. Instrum. Meth. A **506**, 250 (2003).
[26] S. Jadach, B. F. L. Ward and Z. Was, Comp. Phys. Commu. **130**, 260 (2000); Phys. Rev. D **63**, 113009 (2001).
[27] M. Ablikim *et al.*, (BESIII Collaboration), Phys. Rev. D **86**, 092009 (2012).
[28] E. A. Kuraev and V. S. Fadin, Sov. J. Nucl. Phys. **41**, 466 (1985) [Yad. Fiz. **41**, 733 (1985).]
[29] S. Actis *et al.*, Eur. Phys. J. C 66, 585 (2010).
[30] M. Ablikim *et al.* (BESIII Collaboration), Phys. Rev. D **87**, 012002 (2013).
[31] M. Ablikim *et al.* (BESIII Collaboration), Phys. Rev. Lett. **110**,

252001 (2013).
[32] T. Xiao, S. Dobbs, A. Tomaradze and K. K. Seth, Phys. Lett. B **727**, 366 (2013).
[33] M. Ablikim *et al.* (BESIII Collaboration), Phys. Rev. Lett. **112**, 022001 (2014).
[34] K. Zhu, X. H. Mo, C. Z. Yuan and P. Wang, Int. J. Mod. Phys. A **26**, 4511 (2011).
[35] E. V. Abakumova *et al.*, Nucl. Instrum. Meth. A **659**, 21 (2011).
[36] L. Liu *et al.* (Hadron Spectrum Collaboration), J. High Energy Phys. **07**, 126 (2012).
[37] T. Barnes, F. E. Close, and E. S. Swanson, Phys. Rev. D **52**, 5242 (1995); P. Guo, A. P. Szczepaniak, G. Galata, A. Vassallo and E. Santopinto, Phys. Rev. D **78**, 056003 (2008); Yu. S. Kalashnikova and A. V. Nefediev, Phys. Rev. D **77**, 054025 (2008).
[38] M. Cleven *et al.*, Phys. Rev. D **90**, 074039 (2014).
[39] T. W. Chiu and T. H. Hsieh (TWQCD Collaboration), Phys. Rev. D **73**, 094510 (2006).